PNAS RESEARCH ARTICLE | ECOLOGY

Seasonality, density dependence, and spatial population synchrony

Pedro G. Nicolau[a,1], Rolf A. Ims[b], Sigrunn H. Sørbye[a], and Nigel G. Yoccoz[b]

Edited by Alan Hastings, University of California, Davis, CA; received June 15, 2022; accepted November 8, 2022

Studies of spatial population synchrony constitute a central approach for understanding the drivers of ecological dynamics. Recently, identifying the ecological impacts of climate change has emerged as a new important focus in population synchrony studies. However, while it is well known that climatic seasonality and sequential density dependence influences local population dynamics, the role of season-specific density dependence in shaping large-scale population synchrony has not received attention. Here, we present a widely applicable analytical protocol that allows us to account for both season and geographic context-specific density dependence to better elucidate the relative roles of deterministic and stochastic sources of population synchrony, including the renowned Moran effect. We exemplify our protocol by analyzing time series of seasonal (spring and fall) abundance estimates of cyclic rodent populations, revealing that season-specific density dependence is a major component of population synchrony. By accounting for deterministic sources of synchrony (in particular season-specific density dependence), we are able to identify stochastic components. These stochastic components include mild winter weather events, which are expected to increase in frequency under climate warming in boreal and Arctic ecosystems. Interestingly, these weather effects act both directly and delayed on the vole populations, thus enhancing the Moran effect. Our study demonstrates how different drivers of population synchrony, presently altered by climate warming, can be disentangled based on seasonally sampled population time-series data and adequate population models.

population dynamics | spatial ecology | environmental stochasticity | temporal scale dependence | sequential density dependence

Spatial synchrony—referring to the extent local populations display simultaneous changes across space—is a widespread characteristic of geographically distributed populations. The strength and scale of population synchrony, which vary tremendously between species and ecosystems, have been the subject of a large number of theoretical and empirical studies (reviewed by refs. 1 and 2). These studies are motivated by their potential to provide unique insights into the mechanisms that drive ecological dynamics across a range of spatial scales (3–5). The study of spatial population synchrony is one of the fields within ecology that is, both conceptually and methodologically, most tightly linked to other sciences that also deal with spatio-temporal dynamics (6, 7).

P.A.P. Moran developed the first formal theory of spatial population synchrony (8). Moran's theorem postulates that populations subjected to the same regulatory biotic mechanisms (i.e., log-linear density dependence), and influenced by the same abiotic environmental variation (e.g., stochastic weather), will display a synchrony that mirrors the synchrony of the environmental variation (2, 8, 9). While this theorem has become a cornerstone of the study of population synchrony, Moran himself expressed the need for relaxing some of its restrictive assumptions in order to be more applicable to empirical case studies. Subsequently, many studies have contributed to a "generalization of the Moran effect" (sensu 2) by, for instance, allowing for nonlinear density dependence (10, 11), spatially heterogeneous (12, 13) and temporally autocorrelated environmental variation (14), and inclusion of other synchronizing mechanisms [e.g., dispersal (15) and trophic interactions (16)]. Analytical approaches to elucidate the effect of climatic variation on population synchrony have become particularly timely in the current era of anthropogenic climate change (17, 18).

Accounting for seasonality was a fundamental aspect highlighted by Moran when assessing the effect of meteorological conditions on population synchrony (8). This became clear to him when analyzing the population time series of lynx from boreal Canada, which is a region with strikingly different climates in summer and winter. Moran realized that season-specific biotic mechanisms were important because different demographic parameters are involved in the two seasons (e.g., reproduction only in

Significance

Studies of spatial population synchrony have been central to population ecology ever since Patrick Moran's pioneering 1953 paper; however, this field has been deficient in quantitative analyses on how population synchrony can be environmentally forced. The present study provides a novel and widely applicable analytical protocol that allows us to identify how spatial population synchrony is affected by both deterministic (season- and geographic-specific density dependence) and stochastic components (Moran effect). By applying the protocol to seasonally sampled time series of cyclic populations of rodents, we demonstrate how season-specific weather events, likely enhanced by Arctic climate warming, act to affect spatial population synchrony both in a direct and delayed manner.

Author affiliations: [a]Department of Mathematics and Statistics, University of Tromsø-The Arctic University of Norway, N-9037 Tromsø, Norway; and [b]Department of Arctic and Marine Biology, University of Tromsø-The Arctic University of Norway, N-9037 Tromsø, Norway

Author contributions: P.G.N., R.A.I., and N.G.Y. designed research; P.G.N., R.A.I., S.H.S., and N.G.Y. performed research; P.G.N., R.A.I., S.H.S., and N.G.Y. contributed new reagents/analytic tools; P.G.N. analyzed data; and P.G.N., R.A.I., S.H.S., and N.G.Y. wrote the paper.

The authors declare no competing interest.

This article is a PNAS Direct Submission.

[1]To whom correspondence may be addressed. Email: pedrognicolau@gmail.com.

This article contains supporting information online at http://www.pnas.org/lookup/suppl/doi:10.1073/pnas.2210144119/-/DCSupplemental.

Published December 15, 2022.

summer). However, because the lynx population time series were based on only one census per year, Moran was not able to analytically account for season-specific population processes (such as density dependence). More modern studies of seasonally sampled boreal and Arctic rodent populations have shown that marked season-specific density dependence is indeed present and a crucially important determinant of local population dynamics (19–21). Season-specific density dependence is a form of sequential density dependence, which results from demographic or environmental mechanisms which cause density dependence to differ temporally (22, 23). Although seasonality is such a critical aspect of most ecological systems (24), and changing seasonality is one of the most profound consequences of global warming in the northern hemisphere (25), we are not aware of any synchrony study of boreal or Arctic animal populations that has explicitly incorporated seasonality. On the contrary, it has even been argued that one should use annual averages to remove the influence of seasonality when estimating synchrony (e.g., ref. 26).

The purpose of the present study is to devise a general stepwise analytical protocol to identify which aspects of deterministic biotic (density dependence) and stochastic environmental processes (climatic variation) are most influential to spatial population synchrony (detailed in Fig. 1). The protocol applies to settings in which time series of spatially distributed populations are sampled seasonally across ecologically different geographic regions (Steps 1 and 2). The key steps in the analytical protocol correspond to fitting statistical models to the time series that successively account for geographic and seasonal components of the density-dependent structure (Step 3) to understand how these components affect synchrony patterns estimated through correlograms (Step 4). Finally, analyses based on residuals from the best-fitting density-dependent model and spatial synchrony of weather variables are conducted to investigate Moran effects (Step 5). We illustrate the applicability and potential of the protocol through a case study of the gray-sided vole (*Myodes rufocanus*). This boreal-arctic rodent species is renowned for its important role in ecosystem functioning (27) and multiannual population cycles (19, 28), with suspected impacts of climate change on these cycles (29, 30).

Results

Sampling (Step 1). Local gray-sided vole abundances were estimated every spring and fall over 21 y based on capture–recapture sampling in northern Norway (Fig. 2 *A* and *B*). The gray-sided vole has an average lifespan of less than 1 y; it is multivoltine and does not breed during the winter season (31). Sampling in spring was conducted before the recruitment of spring-born voles. Nineteen sampling locations (i.e., live-trapping grids) were spaced along a 170-km transect in a subarctic mountain birch forest and encompassed three predefined geographic regions (R_1: coast, R_2: fiord, and R_3; inland; Fig. 2*A*), which were expected to influence the density-dependent structure of vole population dynamics.

Time Series (Step 2). The 21-y population time series encompass five multiannual cycles, exhibiting profound overall synchrony across the extent of the study area (Fig. 2*B*). However, despite visible spatial synchrony, and relative temporal stationarity, there is also some variation in the timing and amplitude of the cyclic peaks among the localities. This regards especially the spring series (Fig. 2*B*) which have lower and more variable abundance estimates. Moreover, the spring series consist of voles having survived the winter, whereas the fall series are mainly composed of voles recruited over the summer (31).

Previous studies have demonstrated that local boreal and Arctic vole populations are adversely affected by winter weather phenomena, such as thaw–freeze cycles (32, 33) and rain-on-snow events (21). Hence, we derived the local time series of the number of days the temperature crossed zero degrees (Celsius) and the total amount of rainfall (mm) during winter. The two weather variables exhibit spatial synchrony, with a tendency for milder (more zero crosses) and wetter (more rainfall) climates toward the coastal area (Fig. 2 *C* and *D*).

Density-Dependence Structure (Step 3). Following (20), we fitted second-order log-linear autoregressive models to the population time series that successively included annual, geographic, and seasonal components of the density-dependent (DD) structure (Models II–IV, Fig. 1; see *SI Appendix*, Appendix B for estimated model coefficients). As we use a Bayesian framework to conduct the data analysis, we selected Bayesian R^2 (34) as a measure of explained variance (i.e., the fit) of the different linear autoregressive models (see *SI Appendix*, Appendix D for additional information on the Bayesian R^2).

In general, the models explained more of the abundance variance in the fall than the spring (Fig. 3, *Top*). The inclusion of geographic region-specific DD parameters (when comparing II and III) did not improve the model fit much, suggesting that there are small differences in the DD structure between the three geographic regions. However, a large improvement of the model fit was achieved when including season-specific DD parameters (IV), especially concerning the fall abundances. This implies that season-specific biotic DD interactions are strongly influential components of the overall population dynamics and that this season-specific deterministic structure needs to be accounted for (i.e., removed) before assessing the effect of weather variables on the remaining stochastic component (i.e., the residuals from the best fitting model).

Spatial Population Synchrony (Step 4). Population synchrony is here measured by the pairwise Pearson's correlations between population dynamics metrics at different locations. These correlations are then modeled as a function of their respective pairwise distances, providing the pattern of spatial population synchrony in the form of smoothed correlograms (Eq. **4**, Step 4 in *Methods*). The spatial correlograms are displayed in Fig. 3, *Bottom*, based on the four population metrics (I–IV) outlined in Fig. 1 and reveal the contributions of the different DD structure models (II–IV) in explaining the total observed synchrony displayed in correlogram I. The correlograms clearly show that much of the spatial synchrony in the overall abundance dynamics is due to a common season-specific DD structure across the study area. Specifically, when accounting for season-specific DD (Model IV), the synchrony in the residuals drops substantially in comparison to those from Models II and III, which only account for annual DD. The reduction in spatial synchrony due to seasonal DD is particularly sharp for the fall abundances as could have been expected due to Model IV clearly being the best fitting among the models for fall (Fig. 3; *Upper Right*). The correlogram based on residuals from this model (Fig. 3; *Lower Right*) shows that the synchrony between the most distant populations approaches zero, which mirrors the weather synchrony patterns (Fig. 4*A*). Accounting for the slight differences in density dependence among the three geographic

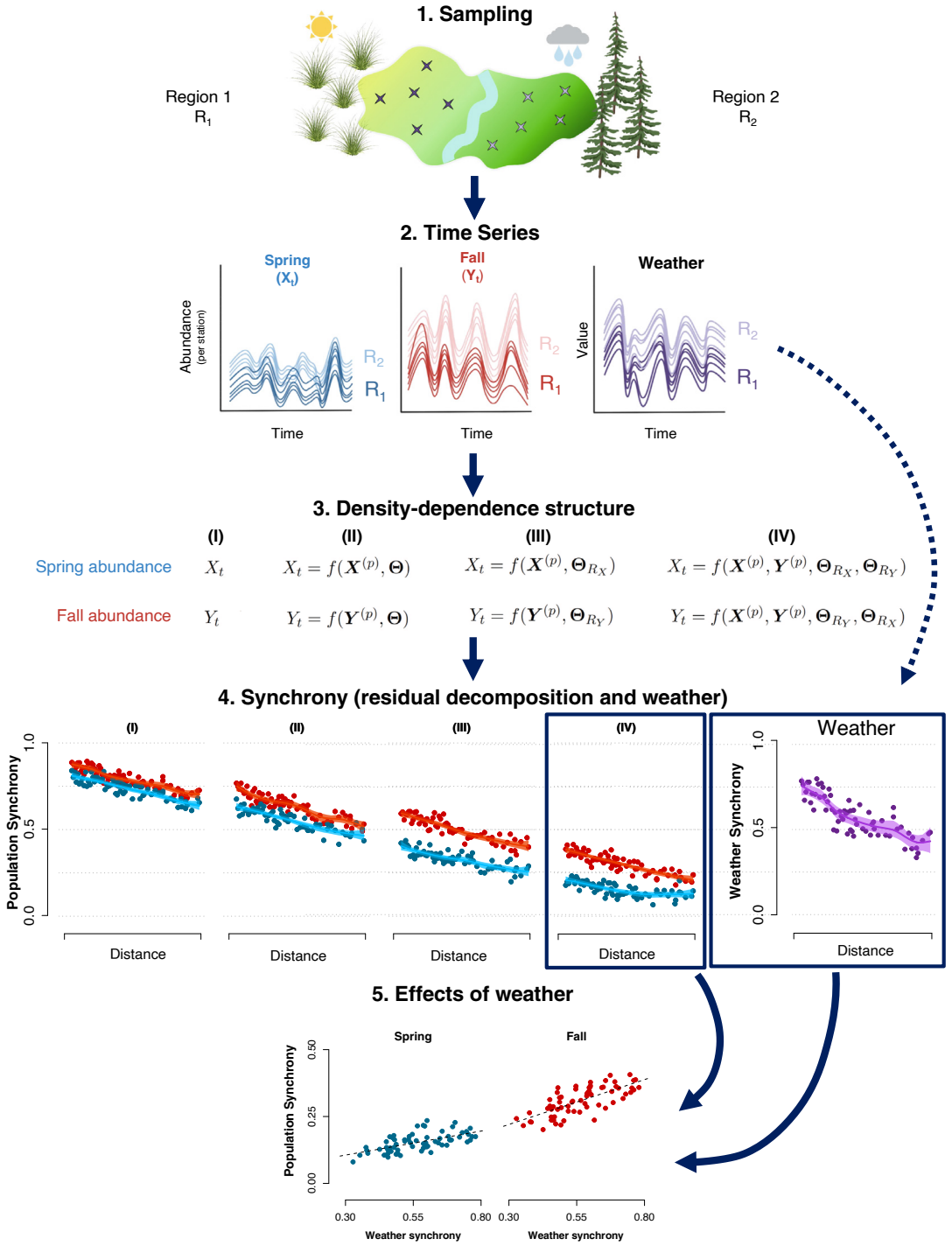

Fig. 1. The five main steps of a general methodological protocol to single out the impacts of climatic variation (weather) on spatial population synchrony, by accounting for seasonal and geographical contexts in ecological population processes (density dependence). Step 1: Seasonal (spring and fall) sampling of both local populations and a focal weather variable at different locations (crosses). The geographic sampling frame encompasses two regions (R_1 and R_2) representing different geographic ecological contexts (e.g., habitats or ecological communities). Step 2: Season- and region-specific time series of local population abundance estimates resulting from the sampling process, together with the time series of the focal weather variable. The estimation of abundance ideally involves separating the observation process and the population process, accounting for detectability. Step 3: Four alternative models to further analyze spatial population synchrony. I) corresponds to seasonal abundance estimates (X_t and Y_t). II–IV) correspond to the sets of residuals $X_t - f(.)$ and $Y_t - f(.)$ from the respective general models for density dependence, modeling the state of the population at time t as a function of the previous p states. Model II includes only one set Θ of density-dependence parameters with annual time lags (i.e., ignoring seasonal and regional components). Model III includes region-specific parameters Θ_R, again with annual time lags (i.e., ignoring seasonal components). Model IV is a bivariate model (20) that includes both geographic- and season-specific parameters Θ_{R_X} and Θ_{R_Y}. Step 4: Season-specific synchrony patterns (i.e., scale and shape) of the population (derived from Step 3) and weather metrics (derived from Step 2) as function of distance. The dots are the pairwise cross-correlations of the population metrics and the weather variables, while the lines are estimated correlograms with associated uncertainty intervals (e.g., 3). Step 5: Estimated effects of weather synchrony on population synchrony. Season-specific (Fall and Spring) population synchrony corrected for seasonal density dependence and geographic context effects (i.e., residuals from Model IV) are regressed against the spatial synchrony in the focal weather variable. Illustrations created with Biorender.com.

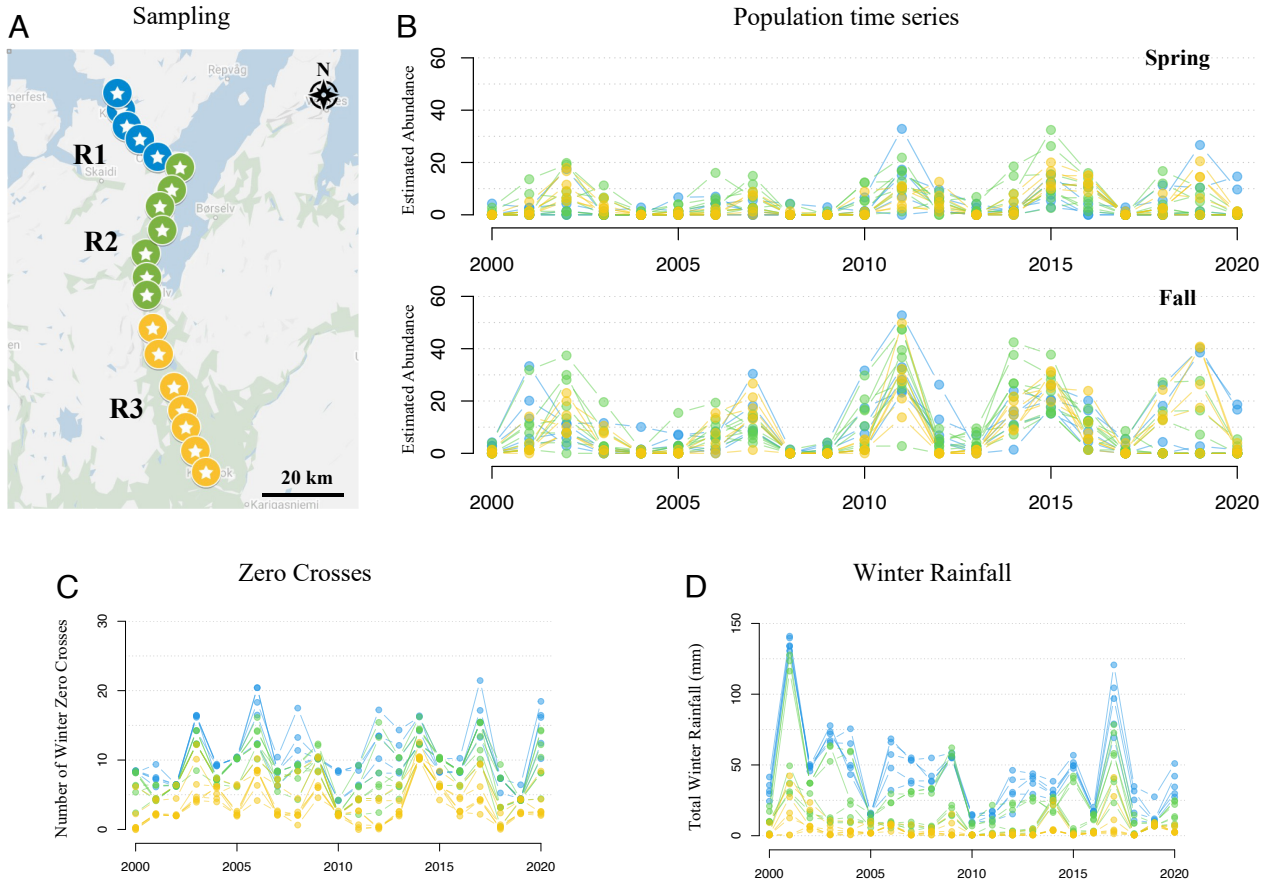

Fig. 2. Sampling design and time series. (*A*) Map with the 19 sampling stations ("dot/stars") along the 170-km transect encompassing three geographical contexts (R_1: coast, R_2: fjord, and R_3: inland). Green shade land cover denotes the mountain birch forest; white denotes tundra and blue denotes water surfaces. (*B*) The time series of abundance estimates for the 19 local gray-sided vole populations in spring (lower) and fall (upper). The time series of the two focal winter weather variables are presented in (*C*) number of zero crossings and (*D*) total winter rainfall. Colors of curves in (*B–D*) correspond to the three geographic contexts in (*A*).

regions provides almost no contribution to the synchrony pattern (i.e., comparison between correlograms II and III).

Effect of Weather (Step 5). The synchrony of both of the weather variables declined steeply as a function of the distance between the sampling stations. However, there was more scattering in the cross-correlations in rainfall when compared to the correlations in the zero crosses (Fig. 4*A*). The synchrony of number of zero crosses was positively and significantly associated with population synchrony corrected for DD structure (Model IV) both in fall and spring, while the synchrony in winter rainfall was only related to the population synchrony in the fall (Fig. 4 *B* and *C*). While the synchrony in the weather variables and the stochastic component of the population fluctuations are significantly related, these empirical relations appear to be weaker than an idealized Moran effect as could be expected from the influence of other stochastic processes than the two weather variables analyzed (2).

Discussion

We have here proposed and exemplified an analytical protocol that, based on time series data, allows for elucidating deterministic and stochastic sources of spatial population synchrony. Potential deterministic sources include density dependence, climatic seasonality, and geographic ecological context, while influential stochastic sources are likely weather variables. Spatial covariance in stochastic weather events amounts to the Moran effect provided that the deterministic components of local population dynamics are linear and identical. Nonetheless, under most circumstances, correlated weather events are expected to also exert synchronizing effects when the local density-dependent structure is nonlinear and spatially and temporally heterogeneous (i.e., the generalized Moran effect; cf. refs. 2, 11, and 12).

Moran showed that a key step to make "meteorological phenomena show up more clearly" in statistical analyses of population synchrony is to remove the density-dependent structure from the population time series before making further statistical inferences (e.g., by analyzing the residuals of an autoregressive model) (8). Many studies have used Moran's approach to remove serial autocorrelation in order to fulfill the independence requirement for significance tests of synchrony (1, 35). However, there appears to be a lack of studies that have followed Moran's suggestion to formally analyze whether the scale of synchrony in the population residuals is dependent on synchrony in the weather (but see ref. 36); i.e., as achieved by Step IV in our analytical protocol. Accordingly, it has been concluded that there has been an "analytical deficiency" in empirical Moran-effect studies in terms of making formal inferences about how population synchrony is environmentally forced (2). We show in the present study that by focusing on residuals, which by definition depend on an adequate model structure, we draw more accurate inferences regarding the strength and scale of

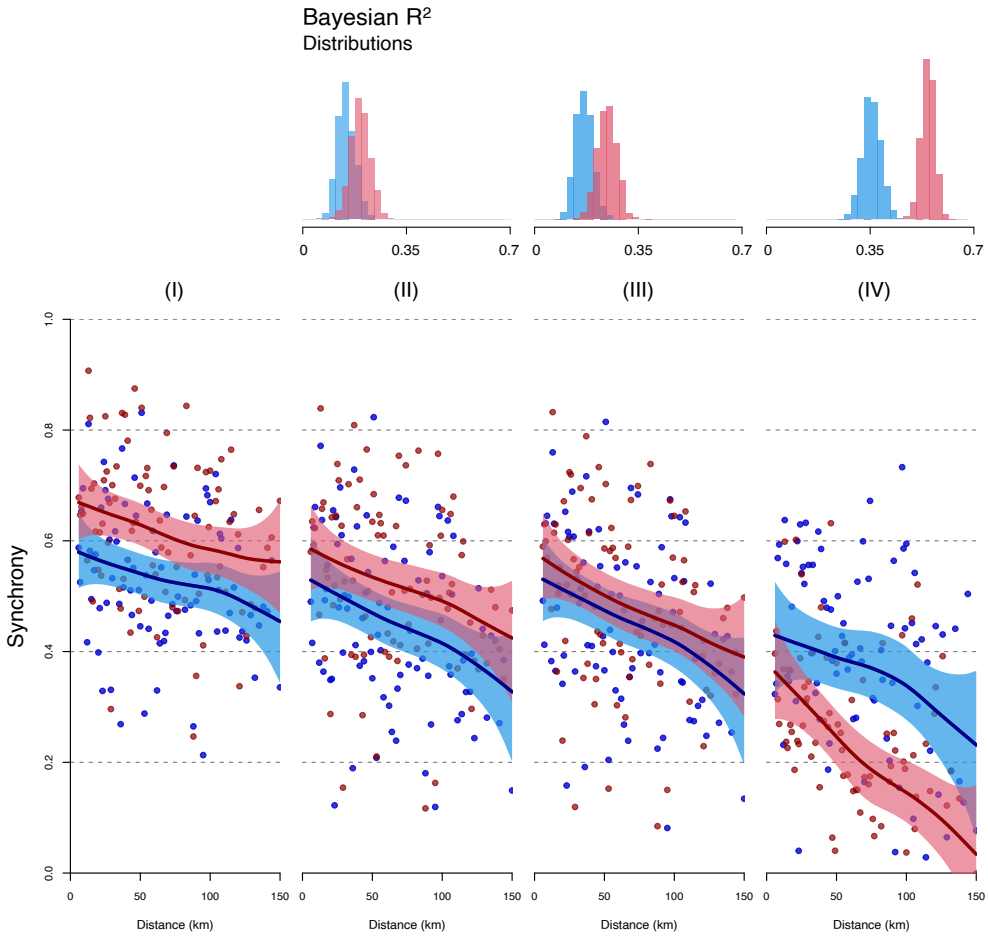

Fig. 3. Modeling and visualizing spatial synchrony. The *Bottom* panels present correlograms displaying how synchrony (i.e., the pairwise spatial correlations) of four different population metrics (see Fig. 1, Step 3) varies with the geographical distance between local gray-sided vole populations. 95% credible intervals for spring are plotted in blue and for fall are plotted in red, while the solid lines correspond to the median. Single dots correspond to the individual pairwise correlations used for the correlogram. The *top* panels display the Bayesian R^2 value distributions with matching color coding, corresponding to the DD Models II–IV. As we are working in a Bayesian framework, the computation of the R^2 results in a distribution itself (*SI Appendix*, Appendix D).

synchrony (37). Indeed, simulations show that not correcting for season-dependent local dynamics, when such is present, leads to biased estimates of synchrony (i.e., inflated correlation of the noise terms; *SI Appendix*, Appendix C).

By applying our analytical protocol to the biannually sampled time series of gray-sided vole populations, we demonstrate winter weather contributions to spatial synchrony. We found that both the amount of rainfall and the frequency of mild spells in winter contribute to spatial synchrony. These two weather variables have previously been found to affect local population dynamics of boreal and arctic vole species by enhancing winter declines (21, 32). However, the present study is the first to analytically link large-scale spatial synchrony in animal populations—a phenomenon that appears to be ubiquitous in boreal and arctic cyclic small rodents (cf. refs. 38 and 39)—to any form of stochastic environmental forcing; i.e., Moran effects.

An interesting result arising from our analysis is the time-lagged effect of the winter weather on the synchrony of fall abundances. Moran found similar time-lagged weather effects on an annual time-scale for Canada lynx and speculated about which biological mechanisms could be involved (8). In voles, environmental conditions in the nonbreeding seasons may have lasting effects, for instance, by delaying the onset of reproduction and thereby reducing population growth over the summer (40). More generally, such environmentally induced carry-over effects represent a kind of cohort effect. Cohort effects have been found to be potentially important to local population dynamics in several animal taxa (41, 42). Our case study suggests that such cohort effects are also likely to cause lagged Moran effects and thereby influence regional population dynamics. The combination of direct and lagged effects of winter weather amounts to enhance the Moran effect as it acts over more than one season. As increased frequencies of rain-on-snow events and thaw–freeze cycles are very likely outcomes of climate warming in boreal and Arctic ecosystems (43), we predict that the strength and scale of spatial synchrony of rodent populations will change in these ecosystems.

Climatic seasonality is an external oscillator that acts strongly on the dynamics of most natural ecological systems (44). Consequently, changed seasonality represents one of the most profound impacts of climate change on ecosystems, especially in boreal and arctic regions (25). Yet, both empirical and theoretical studies of ecological dynamics mostly ignore this fact (24). While seasonality has been shown to be a very important component of spatio-temporal disease dynamics (45–47), we are not aware of empirical studies that have explicitly investigated how such seasonal forcing acts on the strength and scale of synchrony in animal population dynamics. Nevertheless, assessing the role

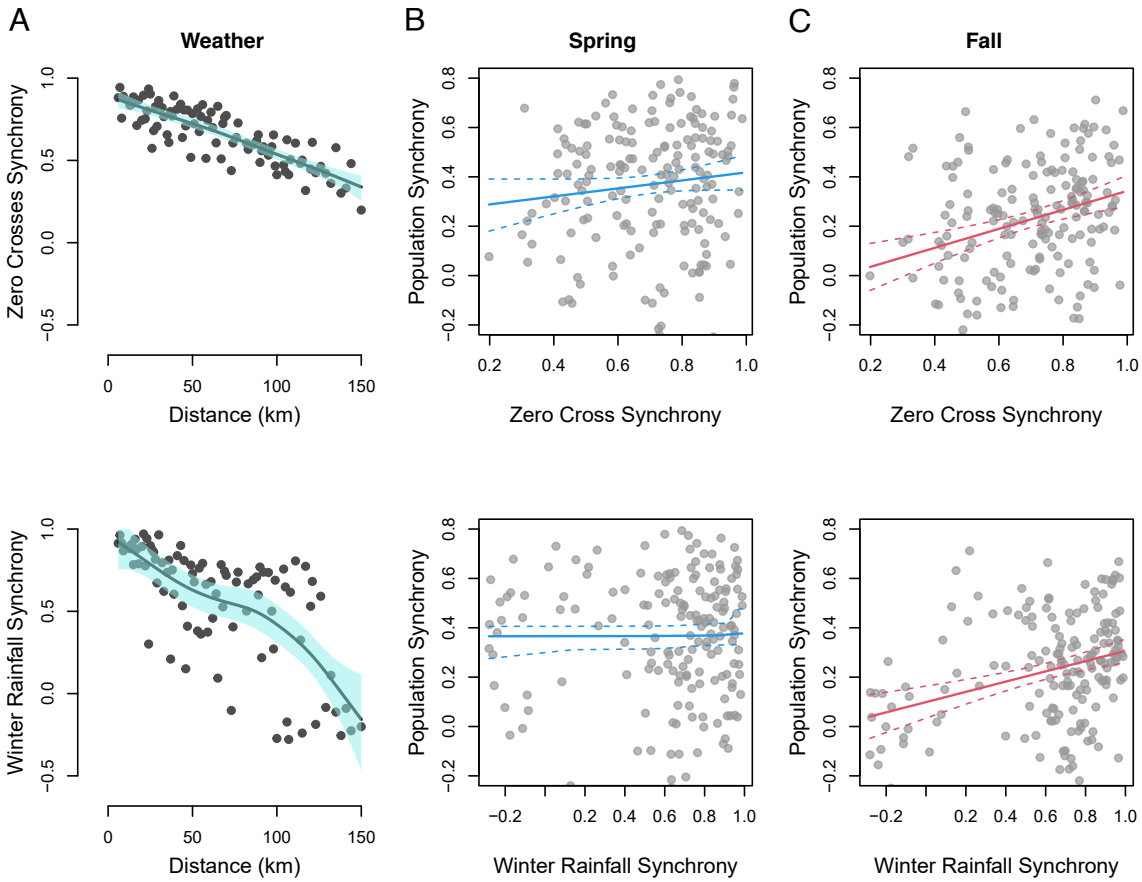

Fig. 4. Weather synchrony vs. population synchrony. Panels (*A*) Correlograms of the two focal weather variables with associated 95% credible intervals, winter zero crosses (ZC; *Top*), and winter rainfall (WR; *Bottom*). Panels (*B*) and (*C*) correspond to linear regression lines, with associated 95% credible intervals, of population synchrony as a function of weather synchrony for spring (*B*) and fall abundances (*C*). Slope estimates for spring are $\beta_{ZC} = 0.16$ (CI = [−0.04, 0.36]) and $\beta_{WR} = 0.00$ (CI = [−0.11, 0.10]). Slope estimates for fall are $\beta_{ZC} = 0.38$ (CI = [0.20, 0.56]) and $\beta_{WR} = 0.21$ (CI = [0.12, 0.30]). CI denotes 95% credible intervals for each of the regression coefficients.

of seasonal dynamics in synchrony studies may be viewed as a particular case of selecting an appropriate temporal scale to elucidate drivers of synchrony (17, 48, 49). Our analytical protocol provides means for assessing the role of such temporal scale dependence. Specifically, the role of seasonality becomes evident by comparing the correlograms of residuals from models with and without seasonal density dependence (i.e., compare correlograms III and IV in Fig. 3). In the case of subarctic gray-sided voles, seasonality is evidently an important determinant of the region-scale spatial synchrony. Especially, this is noticeable for the fall abundances, in which the overall synchrony becomes reduced and the distance effect is enhanced when seasonal density dependence is accounted for. In this case, it appears that the exact nature of such season-specific effects is contingent on the relative magnitude of the spring and fall noise term of the bivariate autoregressive model (*SI Appendix*, Appendix C).

The role of seasonality may be a particularly forceful determinant of spatio-temporal population dynamics in species with multivoltine life cycles, like voles. For instance, the length of winter seasons has been found to exert a strong effect on the local vole population dynamics by acting through a density-dependent structure (20, 50–52) and likely also through season-specific noise terms (53, *SI Appendix*, Appendix C). Moreover, season-specific density dependence is a form of sequential density dependence that may be caused by several biotic mechanisms (22). In boreal and Arctic vole populations, demographic processes are season-specific (e.g., usually no reproduction during winter) so that the resultant population growth rate is likely to exhibit different density dependence in winter and summer (21, 32). Moreover, numerical and functional responses of predators are inherently density dependent and likely to differ between seasons (19). Demographic processes and trophic interactions are typically season-specific also in univoltine species (54)—including how they are affected by density-dependent and independent factors. Hence, we believe that our analytical approach (Fig. 1) will help advance empirical studies of spatial population synchrony for a wide range of species.

Materials and Methods

This section describes how the five steps of the general analytical protocol outlined in Fig. 1 were applied in the gray-sided vole case study.

Sampling (Step 1). We use data collected between 2000 and 2020 from a long-term running monitoring program of the rodent community in the region of Porsanger, northern Norway. The data collection consisted of a capture–mark–recapture methodology with two trapping days at 19 individual stations, scattered along a linear transect of approximately 170 km (Fig. 2). Trapping sessions were conducted over two days twice per year, once in spring (middle of June) and once in fall (middle of September) (see ref. 55 for more details regarding the sampling). Porsanger contains different landscapes that are subject to a strong climatic contrast (in both temperature and precipitation) and likely also biotic contexts (i.e., community structure). The 19 sampling stations were therefore sorted into $m = 3$ regions according to their landscape

affinities (Fig. 2): coastal region (R_1), fjord region (R_2), and inland region (R_3). Stations 1 to 5 were included in R_1 ($n_1 = 5$), stations 6 to 12 were included in R_2 ($n_2 = 7$), and stations 13 to 19 were included in R_3 ($n_3 = 7$). Fig. 2 summarizes spatial features of the study area and data.

Time Series (Step 2).

Abundance Estimation from Mark–Capture–Recapture Data. To reduce a potential bias when estimating synchrony (56), we incorporated the sampling error from capture heterogeneity in our estimates of seasonal abundances (57). Specifically, we fitted a multinomial regression model to the capture history data to estimate the probability of obtaining a given capture history as a function of individual features registered during the live trapping. These features included weight and sex of the individuals. We also added a random effect for the station in the predictor of the regression model. Individual capture probabilities were subsequently estimated by assuming heterogeneous capture probabilities and a temporal effect on the capture process (denoted as model M_{th} in ref. 58). Finally, the individual probabilities were used to estimate seasonal (i.e., spring and fall) abundances using the Horvitz–Thompson estimator (59), which is a function of the estimated individual capture probabilities. We denote the resulting estimated log abundances by $\{X_{s,t}\}$ and $\{Y_{s,t}\}$, for spring and fall, respectively, at spatial locations $s = 1, \ldots, n_s$ and year $t = 1, \ldots, n_t$ (i.e., $n_s = 19$ and $n_t = 21$).

Weather Variables. To explore the effect of the meteorological conditions on the spatial population synchrony, we should ideally look into specific winter snow conditions (i.e., snow depth, hardness, and ice crusts), which are regarded as the most important abiotic variables affecting the population dynamics of boreal and arctic voles (21, 32, 33, 60–62). As such information was not directly available, we resorted to proxy variables of local (i.e., station-specific) snow conditions (cf. refs. 21, 32 and 45), based on modeled daily temperature and precipitation from the Norwegian Meteorological Institute during the years 2000 to 2020. These model-based estimates are more accurate than other climatic gridded datasets, but uncertainties can still be substantial, particularly for precipitation (63). Based on these station-specific temperature and precipitation estimates (detailed in *SI Appendix*, Appendix A), we derived two variables representing locally adverse snow conditions during winter (21 December to 20 March): winter zero crosses (representative of freeze–thaw cycles 32) as the total number of times the mean daily temperature crossed 0 °C; and winter rainfall (representative of rain-on-snow events 62) as the precipitation sum in days where the mean temperature surpassed 0 °C.

Statistical Framework for Decomposing Spatial Synchrony (Steps 3 to 5).

Density-Dependence Structure (Step 3). The general protocol (Fig. 1, Step 3) specifies three different models for the DD structure of the estimated time series. Here, we assume that the general function $f(.)$ is linear, describing the log-DD structure in terms of direct and delayed effects up to lag p. Specifically, the three models either include or exclude regional- and seasonal-dependent effects as specified below.

In general, the sampling locations s are sorted into m regions, $R = R_1 \cup \cdots \cup R_m$. For the gray-sided vole case study, this corresponds to $m = 3$ regions. The most general model includes both regional-specific and seasonal-specific terms (Fig. 1, Model IV), and the assumed log-linear dependency structure up to order p can be expressed by

$$X_{s,t} = \beta_{r1} Y_{s,t-1} + \beta_{r2} X_{s,t-1} + \cdots + \beta_{r,2p-1} Y_{s,t-p} + \beta_{r,2p} X_{s,t-p} + \epsilon_{s,t}, \quad [1]$$

$$Y_{s,t} = \gamma_{r1} X_{s,t} + \gamma_{r2} Y_{s,t-1} + \cdots + \gamma_{r,2p-1} X_{s,t-p+1} + \gamma_{r,2p} Y_{s,t-p} + \omega_{s,t}, \quad [2]$$

where $t = p+1, \ldots, n_t$ and $s \in R_r$. The terms $\epsilon_{s,t}$ and $\omega_{s,t}$ denote individual random environmental noise at each spatial location s for each time point t, while the sets of regional- and seasonal-specific coefficients can be summarized as $\Theta_{R_x} = \{\beta_{r1}, \ldots, \beta_{r,2p}\}$ and $\Theta_{R_y} = \{\gamma_{r1}, \ldots, \gamma_{r,2p}\}$. Simplifications of the given model will yield more simplistic measures of the DD structure. According to the general protocol in Fig. 1, Model (I) corresponds to assuming no DD structure, in which all of the given coefficients are equal to 0. This corresponds to simply using the estimated raw log-abundance series, $\{X_{s,t}\}$ and $\{Y_{s,t}\}$, in further analysis.

Following ref. (20), we included delayed effects up to order $p = 2$ for the case study. Model (II) refers to a second-order annual autoregressive process including coefficients $\Theta = \{\beta_2, \beta_4, \gamma_2, \gamma_4\}$ which are neither regional-specific ($m = 1$; disregarding spatial heterogeneity) nor seasonal-specific ($\beta_1 = \beta_3 = \gamma_1 = \gamma_3 = 0$; assuming yearly dynamics). Such AR(2) models are often used in studies of population synchrony (e.g., refs. 64 and 26). Model (III) is characterized by incorporating regional-specific effects $\{\beta_{r2}, \beta_{r4}, \gamma_{r2}, \gamma_{r4}\}_{r=1}^{m}$. This corresponds to AR(2) models which allow for spatial differences in the DD structure which can account for some of the observed synchrony (13). Finally, by including the seasonal-specific effects $\{\beta_{r1}, \beta_{r3}, \gamma_{r1}, \gamma_{r3}\}_{r=1}^{m}$, we get the bivariate Model (IV) which is very similar to a second-order vector autoregressive model (VAR). The difference to a VAR-model, however, is that the time series $\{X_{s,t}\}$ and $\{Y_{s,t}\}$ are observed at two different time points in year t, and the fall log-abundances are modeled in terms of the spring observations within the same year. Seasonal-specific DD has been recognized as fundamental to model small rodent population dynamics (19), but to our knowledge, seasonal DD contributions to spatial synchrony have not been assessed.

Assessing the Scale and Shape of Spatial Population Synchrony (Step 4). To assess the scale and shape of the spatial synchrony, we can consider the spatial correlations of the environmental noise terms in Models (I–IV) as a function of geographical distance. The following analysis is repeated using the four different models for the DD structure (specified in Step 3, *Materials and Methods*). A major goal is then to understand how the inclusion of region- and season-specific terms influences the synchrony estimates, i.e., which part of the synchrony is explained by the different DD components.

Define the residual vectors $\boldsymbol{\epsilon}'_s = (\epsilon_{s,1}, \ldots, \epsilon_{s,n_t})$ and $\boldsymbol{\omega}'_s = (\omega_{s,1}, \ldots, \omega_{s,n_t})$ for all spatial locations $s = 1, \ldots, n_s$ and $t = p+1, \ldots, n_t$. The contributions to the spatial synchrony are then characterized by the pairwise correlations between vectors within each of the sets $\{\boldsymbol{\epsilon}'_s\}_{s=1}^{n_s}$ and $\{\boldsymbol{\omega}'_s\}_{s=1}^{n_s}$. If the associations between these residual series are expected to be linear, the degree of synchrony is typically measured using Pearson's correlation coefficient (1, 3). To model the correlations in terms of geographical distance, let $\delta_{i,j}$ denote the Euclidean distance between two stations i and j. In accordance with calculating the spatial correlogram (1, 3, 65), we discretize the $n_s(n_s-1)/2$ unique distances between stations into distance classes d_k, $k = 1, \ldots, K$, where K is the total number of classes. Specifically, a distance class d_k is defined by $L_k < \delta_{i,j} < U_k$, where L_k and U_k represent the lower and upper bounds of the distances within that class, respectively. The corresponding averages of the pairwise correlations $\{\rho_{i,j}\}$ for distance class d_k are then given by

$$\rho_k(d_k) = \frac{2\sum_{i=1}^{n_k}\sum_{j=i+1}^{n_k}\rho_{i,j}}{n_k(n_k-1)}, \quad L_k < \delta_{i,j} \le U_k, \quad [3]$$

where n_k is the total number of distances/correlations within distance class d_k. The given formulation is analogous to the calculation of Koenig's modified correlogram (3, 4), as the correlations are not centered (zero synchrony is taken as the reference line of the correlogram). For the given case study, we assumed that the distance-class width is $U_k - L_k = 1$ for all classes, which corresponds to rounding off the geographical distances to the nearest integer. We used this method to calculate the averaged correlations in Eq. 3 as a preprocessing step to reduce random noise in the estimated correlations.

As an alternative to using the nonparametric covariance function (65) or other nonparametric estimates of the correlation function (1), we chose to model the correlations in terms of the distances using the regression model

$$\rho_k(d_k) = f(d_k) + \nu_k, \quad k = 1, \ldots, K. \quad [4]$$

Here, f denotes a smooth underlying function while $\{\nu_k\}$ represents zero-mean, independent Gaussian error terms with constant variance. This model was

here fitted using a Bayesian framework, according to the methodology of integrated nested Laplace approximation (INLA) (66), implemented using the R-package R-INLA (available from http://www.r-inla.org). Specifically, the function f was assigned a second-order intrinsic Gaussian Markov random field prior (67). The model was scaled according to ref. (68), and the precision parameter of the model was assigned a penalized complexity prior with parameters $U = 0.5$ and $\alpha = 0.01$ (69). Using INLA, both the posterior mean and credible intervals for f are calculated efficiently, without the need of resampling techniques, like Monte Carlo simulation or bootstrapping (66).

Effects of Weather (Step 5). Finally, we can use the measures of synchrony accounting for the effects of geographic- and seasonal-dependent DD to investigate potential weather (or other relevant environmental variables) drivers. For this, we can model the set of correlations $\{\rho_k(d_k)\}_{k=1}^{K}$ from Model (IV) as a function of the corresponding spatial correlations of different weather covariates, defined by $\{\rho_k^{(c)}(d_k)\}_{k=1}^{K}$. The availability of such covariates are typically case-specific but should be measured or estimated to represent the same spatial locations and time points used for the log abundance estimates. For the given case study, the relationship between the weather variables (zero crosses and winter rainfall) appeared to be linear and was thus modeled using simple linear regression models.

Data, Materials, and Software Availability. The scripts and supporting data files necessary to replicate this research are available at https://doi.org/10.18710/OVWSAM.

ACKNOWLEDGMENTS. This research was supported by UiT The Arctic University of Norway and is a contribution from the Climate-Ecological Observatory for Arctic Tundra (COAT) through the COAT Tools project.

1. A. Liebhold, W. D. Koenig, O. N. Bjørnstad, Spatial synchrony in population dynamics. *Annu. Rev. Ecol.* **35**, 467–490 (2004).
2. B. B. Hansen, V. Grøtan, I. Herfindal, A. M. Lee, The Moran effect revisited: Spatial population synchrony under global warming. *Ecography* **43**, 1591–1602 (2020).
3. O. N. Bjørnstad, R. A. Ims, X. Lambin, Spatial population dynamics: Analyzing patterns and processes of population synchrony. *Trends Ecol. Evol.* **14**, 427–432 (1999).
4. W. D. Koenig, Spatial autocorrelation of ecological phenomena. *Trends Ecol. Evol.* **14**, 22–26 (1999).
5. J. A. Walter *et al.*, The geography of spatial synchrony. *Ecol. Lett.* **20**, 801–814 (2017).
6. V. R. Nareddy, J. Machta, K. C. Abbott, S. Esmaeili, A. Hastings, Dynamical Ising model of spatially coupled ecological oscillators. *J. R. Soc. Interface* **17**, 20200571 (2020).
7. S. Pérez-García *et al.*, Synchronization of gene expression across eukaryotic communities through chemical rhythms. *Nat. Commun.* **12**, 4017 (2021).
8. P. Moran, The statistical analysis of the Canadian Lynx cycle. 2. Synchronization and meteorology. *Aust. J. Zool.* **1**, 291 (1953).
9. P. J. Hudson, I. M. Cattadori, The Moran effect: A cause of population synchrony. *Trends Ecol. Evol.* **14**, 1–2 (1999).
10. B. Blasius, A. Huppert, L. Stone, Complex dynamics and phase synchronization in spatially extended ecological systems. *Nature* **399**, 354–359 (1999).
11. S. Engen, B. E. Sæther, Generalizations of the Moran effect explaining spatial synchrony in population fluctuations. *Am. Nat.* **166**, 603–612 (2005).
12. T. Royama, Moran effect on nonlinear population processes. *Ecol. Monogr.* **75**, 277–293 (2005).
13. B. Hugueny, Spatial synchrony in population fluctuations: Extending the Moran theorem to cope with spatially heterogeneous dynamics. *Oikos* **115**, 3–14 (2006).
14. T. M. Massie, G. Weithoff, N. Kuckländer, U. Gaedke, B. Blasius, Enhanced Moran effect by spatial variation in environmental autocorrelation. *Nat. Commun.* **6**, 5993 (2015).
15. J. Ripa, Analysing the Moran effect and dispersal: Their significance and interaction in synchronous population dynamics. *Oikos* **89**, 175–187 (2000).
16. J. Jarillo, B. E. Sæther, S. Engen, F. J. Cao-García, Spatial scales of population synchrony in predator-prey systems. *Am. Nat.* **195**, 216–230 (2020).
17. L. W. Sheppard, J. R. Bell, R. Harrington, D. C. Reuman, Changes in large-scale climate alter spatial synchrony of aphid pests. *Nat. Clim. Change* **6**, 610–613 (2015).
18. W. D. Koenig, A. M. Liebhold, Temporally increasing spatial synchrony of North American temperature and bird populations. *Nat. Clim. Change* **6**, 614–617 (2016).
19. T. F. Hansen, N. C. Stenseth, H. Henttonen, Multiannual vole cycles and population regulation during long winters: An analysis of seasonal density dependence. *Am. Nat.* **154**, 129–139 (1999).
20. N. C. Stenseth *et al.*, Seasonality, density dependence, and population cycles in Hokkaido voles. *Proc. Natl. Acad. Sci. U.S.A.* **100**, 11478–11483 (2003).
21. D. Fauteux, A. Stien, N. G. Yoccoz, E. Fuglei, R. A. Ims, Climate variability and density-dependent population dynamics: Lessons from a simple High Arctic ecosystem. *Proc. Natl. Acad. Sci. U.S.A.* **118**, e2106635118 (2021).
22. I. I. Ratikainen, J. A. Gill, T. G. Gunnarsson, W. J. Sutherland, H. Kokko, When density dependence is not instantaneous: Theoretical developments and management implications. *Ecol. Lett.* **11**, 184–198 (2008).
23. M. Åström, P. Lundberg, S. Lundberg, Population dynamics with sequential density-dependencies. *Oikos* **75**, 174 (1996).
24. E. R. White, A. Hastings, Seasonality in ecology: Progress and prospects in theory. *Ecol. Complex.* **44**, 100867 (2020).
25. L. Xu *et al.*, Temperature and vegetation seasonality diminishment over northern lands. *Nat. Clim. Change* **3**, 581–586 (2013).
26. T. A. Dallas, L. H. Antão, J. Pöyry, R. Leinonen, O. Ovaskainen, Spatial synchrony is related to environmental change in Finnish moth communities. *Proc. R. Soc. Lond. B Biol. Sci.* **287**, 20200684 (2020).
27. R. Boonstra *et al.*, Why do the boreal forest ecosystems of northwestern Europe differ from those of western North America? *BioScience* **66**, 722–734 (2016).
28. P. Turchin, L. Oksanen, P. Ekerholm, T. Oksanen, H. Henttonen, Are lemmings prey or predators? *Nature* **405**, 562–565 (2000).
29. R. A. Ims, J. A. Henden, S. Killengreen, Collapsing population cycles. *Trends Ecol. Evol.* **23**, 79–86 (2008).
30. T. Cornulier *et al.*, Europe-wide dampening of population cycles in keystone herbivores. *Science* **340**, 63–66 (2013).
31. Y. Kaneko, K. Nakata, T. Saitoh, N. C. Stenseth, O. N. Bjørnstad, The biology of the vole Clethrionomys rufocanus: A review. *Popul. Ecol.* **40**, 21–37 (1998).
32. J. Aars, R. A. Ims, Intrinsic and climatic determinants of population demography: The winter dynamics of tundra voles. *Ecology* **83**, 3449–3456 (2002).
33. K. L. Kausrud *et al.*, Linking climate change to lemming cycles. *Nature* **456**, 93–97 (2008).
34. A. Gelman, B. Goodrich, J. Gabry, A. Vehtari, R-squared for Bayesian regression models. *Am. Stat.* **73**, 307–309 (2019).
35. J. P. Buonaccorsi, J. S. Elkinton, S. R. Evans, A. M. Liebhold, Measuring and testing for spatial synchrony. *Ecology* **82**, 1668–1679 (2001).
36. V. Grøtan *et al.*, Climate causes large-scale spatial synchrony in population fluctuations of a temperate herbivore. *Ecology* **86**, 1472–1482 (2005).
37. M. Lillegård, S. Engen, B. E. Saether, Bootstrap methods for estimating spatial synchrony of fluctuating populations. *Oikos* **109**, 342–350 (2005).
38. N. C. Stenseth, R. A. Ims, "Population dynamics of lemmings: Temporal and spatial variations" in *The Biology of Lemmings*, N. C. Stenseth, R. A. Ims, Eds. (Academic Press, 1993), pp. 61–97.
39. C. J. Krebs, *Population Fluctuations in Rodents* (University of Chicago Press, 2013).
40. M. J. Smith, A. White, X. Lambin, J. A. Sherratt, M. Begon, Delayed density-dependent season length alone can lead to rodent population cycles. *Am. Nat.* **167**, 695–704 (2006).
41. J. M. Gaillard *et al.*, How does climate change influence demographic processes of widespread species? Lessons from the comparative analysis of contrasted populations of roe deer. *Ecol. Lett.* **16**, 48–57 (2013).
42. J. F. Le Galliard, O. Marquis, M. Massot, Cohort variation, climate effects and population dynamics in a short-lived lizard. *J. Anim. Ecol.* **79**, 1296–1307 (2010).
43. A. M. A. P., Snow, Water, Ice and Permafrost in the Arctic (SWIPA) 2017. Arctic Monitoring and Assessment Programme (AMAP), Oslo, Norway. xiv+ (2017), p. 269.
44. S. D. Fretwell, *Populations in a Seasonal Environment* (Princeton University Press, Princeton, 1972).
45. D. J. Earn, P. Rohani, B. T. Grenfell, Persistence, chaos and synchrony in ecology and epidemiology. *Proc. R. Soc. Lond. B Biol. Sci.* **265**, 7–10 (1998).
46. B. T. Grenfell, O. N. Bjørnstad, J. Kappey, Travelling waves and spatial hierarchies in measles epidemics. *Nature* **414**, 716–723 (2001).
47. A. Moustakas, M. R. Evans, I. N. Daliakopoulos, Y. Markonis, Abrupt events and population synchrony in the dynamics of bovine tuberculosis. *Nat. Commun.* **9**, 2821 (2018).
48. T. L. Anderson *et al.*, The dependence of synchrony on timescale and geography in freshwater plankton. *Limnol. Oceanogr.* **64**, 483–502 (2018).
49. L. G. Shoemaker *et al.*, The long and the short of it: Mechanisms of synchronous and compensatory dynamics across temporal scales. *Ecology* **103**, e3650 (2022).
50. G. O. Batzli, Can seasonal changes in density dependence drive population cycles? *Trends Ecol. Evol.* **14**, 129–131 (1999).
51. N. C. Stenseth, Population cycles in voles and lemmings: Density dependence and phase dependence in a stochastic world. *Oikos* **87**, 427 (1999).
52. S. M. Bierman *et al.*, Changes over time in the spatiotemporal dynamics of cyclic populations of field voles (*Microtus agrestis* L.). *Am. Nat.* **167**, 583–590 (2006).
53. D. A. Vasseur, Environmental colour intensifies the Moran effect when population dynamics are spatially heterogeneous. *Oikos* **116**, 1726–1736 (2007).
54. M. S. Boyce, A. R. E. Sinclair, G. C. White, Seasonal compensation of predation and harvesting. *Oikos* **87**, 419 (1999).
55. D. Ehrich, N. G. Yoccoz, R. A. Ims, Multi-annual density fluctuations and habitat size enhance genetic variability in two northern voles. *Oikos* **118**, 1441–1452 (2009).
56. H. Santin-Janin *et al.*, Accounting for sampling error when inferring population synchrony from time-series data: A Bayesian state-space modelling approach with applications. *PLoS ONE* **9**, e87084 (2014).
57. P. G. Nicolau, S. H. Sørbye, N. G. Yoccoz, Incorporating capture heterogeneity in the estimation of autoregressive coefficients of animal population dynamics using capture–recapture data. *Ecol. Evol.* **10**, 12710–12726 (2020).
58. D. L. Otis, K. P. Burnham, G. C. White, D. R. Anderson, Statistical inference from capture data on closed animal populations. *Wildl. Monogr.* **62**, 3–135 (1978).
59. D. G. Horvitz, D. J. Thompson, A generalization of sampling without replacement from a finite universe. *J. Am. Stat. Assoc.* **47**, 663–685 (1952).
60. L. Hansson, H. Henttonen, Gradients in density variations of small rodents: The importance of latitude and snow cover. *Oecologia* **67**, 394–402 (1985).
61. B. B. Hansen *et al.*, Climate events synchronize the dynamics of a resident vertebrate community in the high arctic. *Science* **339**, 313–315 (2013).
62. A. Stien *et al.*, Congruent responses to weather variability in high arctic herbivores. *Biol. Lett.* **8**, 1002–1005 (2012).
63. C. Lussana, O. E. Tveito, A. Dobler, K. Tunheim, seNorge_2018, daily precipitation, and temperature datasets over Norway. *Earth Syst. Sci. Data* **11**, 1531–1551 (2019).
64. T. Turkia *et al.*, Large-scale spatial synchrony in red squirrel populations driven by a bottom-up effect. *Oecologia* **192**, 425–437 (2020).

65. O. N. Bjørnstad, W. Falck, Nonparametric spatial covariance functions: Estimation and testing. *Environ. Ecol. Stat.* **8**, 53–70 (2001).
66. H. Rue, S. Martino, N. Chopin, Approximate Bayesian inference for latent Gaussian models by using integrated nested Laplace approximations. *J. R. Stat. Soc. Series B Stat. Methodol.* **71**, 319–392 (2009).
67. H. Rue, L. Held, *Gaussian Markov Random Fields: Theory and applications* (Chapman and Hall/CRC, 2005).
68. S. H. Sørbye, H. Rue, Scaling intrinsic Gaussian Markov random field priors in spatial modelling. *Spat. Stat.* **8**, 39–51 (2014).
69. D. Simpson, H. Rue, A. Riebler, T. G. Martins, S. H. Sørbye, Penalising model component complexity: A principled, practical approach to constructing priors. *Stat. Sci.* **232**, 1–28 (2017).